An Absorber-Integrated Taper Slot Antenna

Jiyu Wu, *Member, IEEE*, Yihong Qi, *Senior Member, IEEE*, Wei Yu, *Member, IEEE*, Lie Liu, *Senior Member, IEEE*, and Fuhai Li, *Member, IEEE*

***Abstract*—The characteristic of quiet zone is essential for anechoic chambers that have been extensively used in the over-the-air tests. Multireflection in the anechoic chambers of the probe antennas could deteriorate the quiet zone and hence limit the capability of systems to detect small signals, throughput of multiple-input and multiple-output and radio frequency parameter measurement. In this paper, the authors developed an integrated approach of antenna-absorber codesign for a taper slot antenna (TSA) with low radar cross section (RCS). Low RCS antenna minimizes the reflection coefficient of the sampling antennas, the building block of anechoic chamber. This antenna is composed of an open-boundary TSA and shaped expanded polypropylene absorbers that surround the antenna. This new type of hybrid TSA is typically designed for anechoic chamber working from 0.6 to 6 GHz. The measured boresight reflectivity of the hybrid antenna has been achieved at least –27 dB from 0.6 to 6 GHz.**

***Index Terms*—Broadband antennas, over-the-air (OTA), radar absorbing material, radar cross sections (RCS), sensitivity, vivaldi antennas.**

I. Introduction

MULTIPLE-INPUT multiple-output (MIMO) plays an important role in improving capacity and reliability of wireless communication network and become an essential part of communications standards, such as long term evolution and coming fifth generations mobile network (5G). In order to evaluate MIMO devices and systems, the Cellular Telecommunication and Internet Association, and the Third Generation Partnership Project (3GPP), have been pushing for MIMO over-the-air (OTA) test standardization for years [1], [2]. The antenna and RF test chambers are commonly used for OTA test. Multiprobe antenna chambers have been widely used to speed up the antenna test time. The multiprobe chambers are utilized to provide a multisource environment to simulate MIMO multipath channel modeled by means of combined effort of channel emulator and chamber hardware, which is called multiprobe anechoic chamber method (MPAC). Radiated two-stage method (RTS) in 3GPP standard can also perform MIMO OTA test, using RTS in multiprobe chambers can make the measurement process more efficient and easier for the search of invert matrix [3], [4].

In multiprobe chamber system design, the sampling antennas (SAs) are playing an important role. For the multiprobe antenna chamber or single-input and single-output OTA test, the quiet zone is going to affect antenna side lobe and null measurement accuracy and OTA measurement uncertainty [5]–[7]. For RTS MIMO OTA tests, the quiet zone ripple level could add noisy weighting to the accredit channel model and increase throughput test uncertainty. For OTA RF performance testing, the quiet zone ripple can cause error vector magnitude measurement error. Chamber design and improvement of the absorption rate of the absorbers are the means for solving quiet zone ripple problems. The SA or probe antenna and the SA arrangement in multiprobe chamber are factors that have to be considered in ultra-low quiet zone ripple chamber design. In MPAC SA isolation is also needed to be taken care of. Therefore, the SA should be with narrow beamwidth and low radar cross section (RCS) or reflectivity with radar absorbing material (RAM). This scattering performance can be characterized by RCS and reflection coefficient. Yet the probe antennas with low RCS in anechoic chambers have not been published based on our best knowledge.

RCS is defined by the ratio of reflected to incident power as follows:

$$\sigma = \lim_{R\to\infty} 4\pi R^2 \frac{\left|E_s^2\right|}{\left|E_i^2\right|} \tag{1}$$

where σ is the projected area of a metallic sphere that would scatter as same power as the target does in the same direction, *R* is the distance between the target and the source, and *Es* and *Ei* are the strength of the scattered and incident electric fields, respectively. The reflection coefficient or the reflectivity of the RAM is also defined by the ratio of reflected to incident power, $R = P_{\mathrm{re}}/P_{\mathrm{in}}$.

The factors that contribute to the RCS of antennas can be categorized into two parts: structural mode and antenna mode [8]. The first mode scattering from the incident field comes from the shape, size, and materials. The second one is the reradiation of the incident field that received by the antenna. In the structural mode, since antennas are mostly composed of metallic material, its scattering performance depends on its shape and size. The antenna of pointed shape and small size may have a lower RCS in a wideband. Also in the antenna mode, the incident electromagnetic wave can generate induced current on the surface of antennas. The induced current flows through the radiator, the transmission line, and finally reaches the systems that connected to the antennas. Any reflection in this process

Manuscript received May 2, 2017; accepted May 25, 2017. Date of current version August 17, 2017. This work was supported by the Chinese Ministry of Education–China Mobile Research Foundation under Grant MCM 20150101. *(Corresponding author: Jiyu Wu.)*

J. Wu, W. Yu, and L. Liu are with Hunan University, Changsha 410082, China, and also with General Test Systems, Shenzhen 518102, China (e-mail: jiyu.wu@generaltest.com; fred.yu@generaltest.com; lie.liu@generaltest.com).

Y. Qi is with General Test Systems, Shenzhen 518102, China, also with Hunan University, Changsha 410082, China, and also with the Missouri University of Science and Technology, Zhuhai 519000, China (e-mail: Yihong.qi@generaltest.com).

F. Li is with Hunan University, Changsha 410082, China (e-mail: fuhai-li@vip.sina.com).

Color versions of one or more of the figures in this paper are available online at http://ieeexplore.ieee.org.

Digital Object Identifier 10.1109/TEMC.2017.2714580

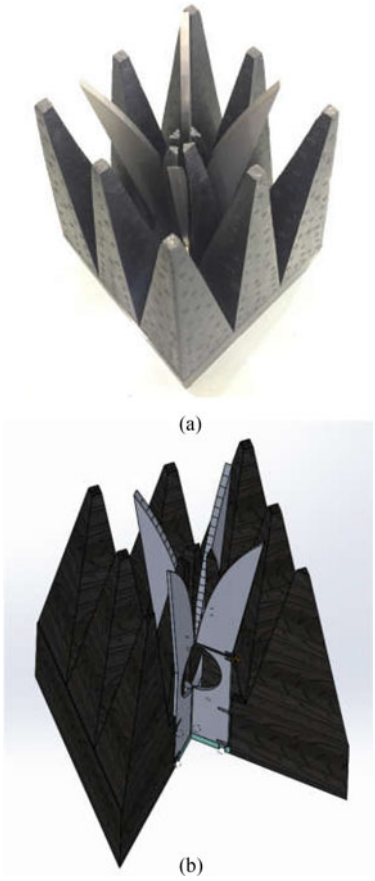

Fig. 1. Absorber-integrated TSA. (a) The TSA with absorber covering 0.6–6 GHz. (b) The detail view of the antenna.

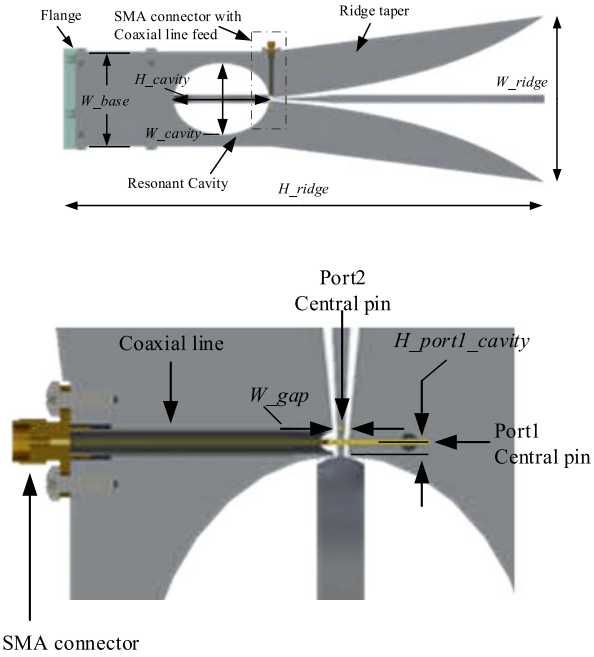

Fig. 2. Cross section views of the antenna.

could reradiate back to the space, and increase the RCS of the antennas. Therefore, low VSWR and matched load can help to reduce a wideband RCS resulted from the antenna mode.

Many techniques have been applied to reduce the RCS of antennas, including using traditional pyramidal RAM [8], metamaterial [9], and other absorbing materials [10]. However, it has not been reported about probe antennas that has wideband reduction of RCS for anechoic chambers.

In anechoic chamber design, reflection coefficient or reflectivity are usually used to characterize the performance of the absorbers, the building blocks of the chambers. In single-probe chambers, the quality of the quiet zone generally depends on the reflection properties of RAM and the scattering performance of the probe antenna that influences the multireflection between the probe and the device-under-test. In multiprobe chambers, the multireflection between probes becomes a bottleneck of the quiet zone.

Our goal is to develop a kind of taper slot antenna (TSA), as shown in Fig. 1, that integrated with absorber in anechoic chambers, with minimized reflection coefficient and RCS.

II. Design of a TSA With Low RCS

A. Taper Slot Antennas

The first reported TSA was developed by Gibson [11], which was also called as the Vivaldi antenna. The TSA has been extensively used as the measurement antenna due to its wideband performance and high directivity. Generally, an endfire TSA consists of an antenna feed, a resonant cavity, and a tapered slot radiator, as shown in Fig. 2.

Since test systems are usually required to measure two orthogonal polarizations, namely horizontal and vertical polarization, the probe antennas are composed of a pair of TSA elements. These two TSA elements mechanically connect with each other perpendicularly but isolate electrically in radio path of the antennas. The orthogonally mechanical arrangement ensures high polarization purity in the antenna's boresight direction. The two TSA elements are often designed with similar mechanical and electrical properties with a little difference in the central pins, as shown in Fig. 2, to maintain symmetric patterns and high isolation between two ports.

TSA, as an endfire antenna, is designed to radiate the electromagneticpower in the boresight direction with low VSWR. The central pin, soldered with a 50 ΩSMA connector, was mechanically fixed to its opposite ridge. This feed configuration will excite quasi-TEM mode along the slot line in both directions, while the resonant cavity, working as an open end, suppresses the current flowing down to the bottom of the antenna. Therefore, the most energy will travel to the antenna boresight direction and radiate. This quasi-TEM mode makes the TSA a wideband antenna, and the design of resonant cavity has a great impact on the VSWR, the RCS, and the bandwidth of the TSA.

The tapered ridges with flared curve extended to open space work as a radiator. The length and the width of the ridge and the profile of the curve determine the gain, the beamwidth, and the VSWR of the antenna. The general design guide can be find in [12].

TSA is usually composed of bilateral slot lines on the surface of a substrate. Although this configuration is cost effective, the printed circuit board (PCB) based antenna design also brings in

challenges of mechanical fabrication and antenna efficiency. As mentioned above, the probe antennas consist of two TSA elements that orthogonally fix with each other. Since the thickness of the PCB-based antenna can hardly exceed 3 mm, it is difficult to maintain high assembly accuracy for the orthogonal fixing without the help of other customized fixtures. In addition, the dielectric loss from the substrate of the PCB deceases the antenna efficiency and gain which can barely be controlled, especially in high frequency over 3 GHz. Therefore, the proposed TSA are made up of aluminum-alloy-based material that mechanically fabricated by using computer numerical control (CNC). In this way, the assembly errors and the dielectric loss can be minimized.

B. TSAs With Low RCS

The general recent research about reducing RCS of antennas includes radar absorbing method [9], surface current reconfiguration [13], and scattering reduction [8]. In the radar absorbing method, the RCS performance of antennas greatly depend on the properties of the RAM. For example, the electromagnetic bandgap absorbers can be applied to reduce the patch antennas' RCS [14]. Due to the resonant nature of the electromagnetic bandgap absorbers, the bandwidth of this method may be challenging. By using surface current reconfiguration method, antennas are modified and optimized to limit the surface current that induced by the incident electromagnetic waves in certain directions. However, the RCS reduction is limited in this method compared to the RAM way.

From the theory of antenna RCS reduction [8], as have been mentioned above, the antenna RCS is composed of antenna mode RCS and structural mode RCS. To lower the antenna mode RCS, the antenna should be designed with lower VSWR, and the antenna should be connected with a match terminal. As an electromagnetic receiver and radiator, antennas receive the incident electromagnetic waves, and the induced current mostly concentrates on the areas of radiator and transmission lines to the antenna connector. Any discontinuities along this path can cause the reflection of the incident current, and reradiate back to the space, which in turn higher the RCS of the antenna. By lowering the VSWR of the antenna, and terminating the antenna with a match load, the incident waves can be absorbed by the terminal with minor reflection and thus the RCS could be greatly reduced.

Another factor that can greatly influence the RCS of antennas is the structural mode RCS. The main approach to reduce the structural mode RCS is shaping [8]. The principle of shaping is to minimize the RCS in important direction by scattering the fields to the unimportant direction. In the case of probe antennas design, though shaping could not reduce the overall RCS or reflectivity of the probe antennas, it can redirect the scattering waves to the absorbers instead of to the quiet zone of chambers.

By applying these RCS reduction methods mentioned above, a wideband probe antenna with low RCS and reflectivity is designed to integrate the probe antennas with the RAM, lower the VSWR of the antenna, and to optimize the shape.

C. RAM Absorbers

The RAM used in the proposed antenna is VICREAT's DURA EM absorber, whose height is 380 mm. As shown in Figs. 1 and 7, the absorber has the pyramidal shape, where the height of the cuboidal base is 100 mm, the width of the base is 80 mm, and the top of the pyramid is a 10 mm $\times$ 10 mm square. This kind of RAM employs expanded polypropylene (EPP) as holding matrix and nano carbon black as absorbent. EPP foam is a light, mechanically robust, and close-cell material with good solvent and chemical resistance.

TABLE I
DETAILS OF THE COMPLEX PERMITTIVITY VERSUS FREQUENCY

Frequency (GHz)	The real part of the permittivity	The imaginary part of the permittivity
1.7	2.30	3.29
3	2.00	2.03
5.84	1.77	1.25

The principle of the RAM is absorbing incident electromagnetic waves by impedance matching to the impedance of the free space. The impedance matching condition could be determined by the dielectric properties and structure of the RAM. The dielectric properties include the complex relative permittivity $\varepsilon_r^* = \varepsilon_r' - j\varepsilon_r''$ and the complex relative permeability $\mu_r^* = \mu_r' - j\mu_r''$, where ε' and μ' are the real parts, and ε'' and μ'' are the imaginary parts. The complex permeability of the RAM used in the proposed antenna stays unity since no magnetic material is used. The measured complex permittivity is shown in Table I. The dispersion of its complex permittivity is represented by the Debye equation [15].

The EPP absorbers have several advantages over the traditional ones such as mechanically robust and close-cell materials. One of the traditional absorbers that have been widely used in chambers is polyurethane (PU) absorber. Since the conventional PU absorber is too soft mechanically to be precisely machined or mold fabricated, it is difficult to design a PU absorber-integrated antenna with low fabrication error. However, EPP absorbers can be fabricated using CNC machining and mold fabrication, which can limit the fabrication error in 1 mm. In addition, since the PU absorbers are of open-cell material and mechanical fabrication could break the PU absorbers and release the absorbents. Fabrication such as hot wire cutting could adversely affect the performance of the absorbers. However, the absorbing performance of EPP absorbers can be stable after mechanically fabrication for its close-cell materials. Therefore, EPP absorber is a better candidate for the proposed absorber-integrated antenna design.

D. Design of the Low RCS TSA

As shown in Fig. 1, the TSA was arranged to place inside a pyramid with 45° rotation. This rotation resulted from the absorber configuration in Rayzone 2800 from General Test System, for which the proposed antennas have been designed. This absorber configuration of 45° rotation bettered the performance of Rayzone 2800 chambers.

A prototype was designed and fabricated, as shown in Figs. 1 and 2. The total length of the antenna *H_ridge* is 395 mm; the maximum width *W_ridge* between two ridges around the aperture is 140 mm; the width of base *W_base* is 80 mm; and the thickness of the ridge is 7 mm. The gap *W_gap* between two

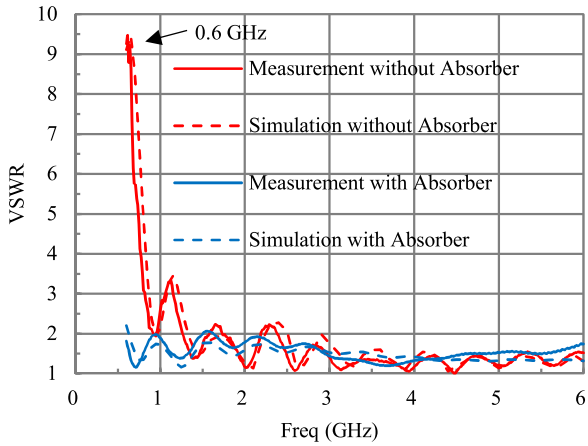

Fig. 3. Measured and simulated VSWR of the antenna.

slot line at the feed points is 2 mm. The curve of the ridge taper is applied with an exponential equation as follows:

$$x = W\_gap + (W\_ridge - W\_gap)\frac{\exp(\alpha y/H\_ridge) - 1}{(\exp(\alpha) - 1)} \tag{2}$$

where α is to control the slope of the exponential curve. This slot line with exponential curve has the advantage of larger bandwidth compared to the linear curve.

In the area of feeding, in Fig. 2, the distance between the port1 central pin and the top edge of the resonant cavity *H_port1_cavity* is 1 mm; the port2 central pin is vertically placed 1 mm higher than the port1 central pin; the width of the ellipsoidal resonant cavity *W_cavity* is 60 mm, and the height *H_cavity* is 80 mm. These arrangements are based on the consideration for both VSWR and mechanical feasibility.

In order to optimize the RCS of the absorber-integrated TSA, some special designs have been applied. The TSA is placed inside a cut pyramidal absorber with only 3 mm space between them. This configuration could detune the TSA, thus lower the VSWR at low frequency, and it can also limit the induced current generated by the incident electromagnetic wave, which in turn reduces the RCS. The structure of the radiator has also been optimized. Although with larger *W_ridge*, the antenna could obtain a bigger aperture, and a higher gain, the RCS of the antenna would be increased for its more observing area. The end of the ridge was also designed to be a point end instead of an edge end to reduce the RCS from the edge diffraction.

E. Simulation Results of the Low RCS TSA

The simulation results are shown in Figs. 3–6. The simulated VSWR is decreased in the low frequency due to the detuning of RAM. The VSWR for different ports are of little difference, so only the VSWR of one port is shown for simplicity.

In Fig. 4, though the gain of the TSA with integrated RAM is decreased compared to the TSA without RAM, the RCS will also be reduced, because antenna mode RCS is proportional to the gain of the antenna [8]. The reduction of the gain and the efficiency of the RAM integrated TSA has little impact on the performance of anechoic chamber systems because adequate

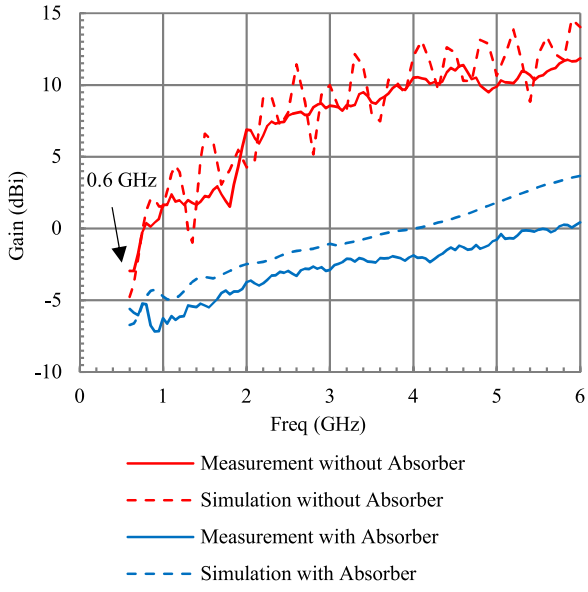

Fig. 4. Measured and simulated boresight gain of the TSA.

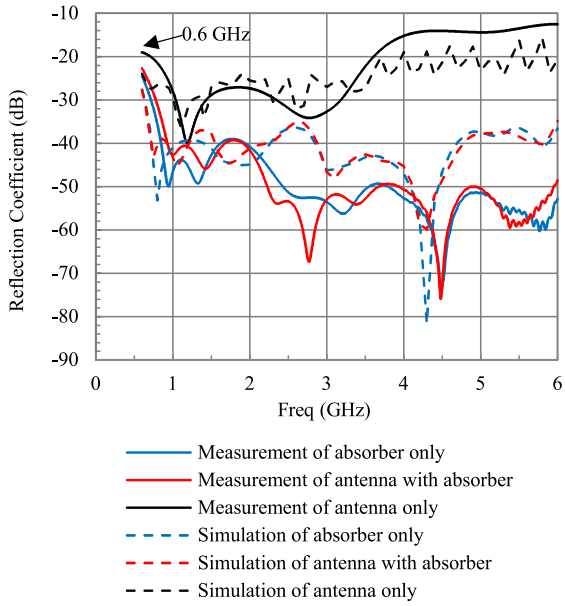

Fig. 5. Reflection coefficient measurement and simulation results of TSA with absorber, absorber only, and antenna only.

link budget can be achieved by controlling path loss and adding low noise amplifier in the chamber system design. In addition, because the two TSA connected to port1 and port2 have the same radiator structure, the simulated gain for port1 and port2 are of same results.

The reflection coefficient is simulated by calculating the S_{11} of the port, where a uniform plane wave is excited and perpendicularly applied on the infinitely large periodic absorbers. Periodic boundaries are often used to realize the infinite size of the absorbers and simplify the mesh. As shown in Fig. 5, the reflection coefficient was simulated to evaluate the influence of the antenna on the absorber, and the results showed the designed TSA with low RCS changed little on the reflectivity of

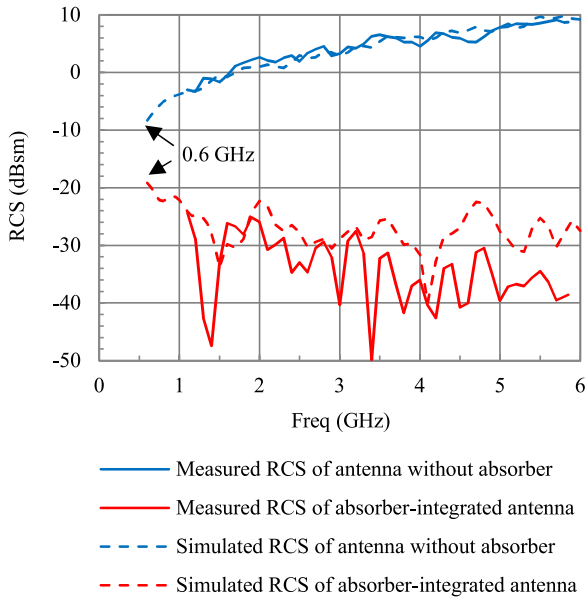

Fig. 6. RCS of the proposed TSA with and without absorbers.

the absorber. By comparing the absorber-integrated TSA with absorber-free TSA, the importance of RAM in the proposed antenna is shown, and typically about 15 dB reflection coefficient reduction was contributed by the absorbers.

And in Fig. 6, the monostatic RCS in the gazing direction was reduced by at least 10.9 dB in a wideband from 0.6 to 6 GHz. The RCS reduction effect grows as the frequency increases.

III. Fabrication and Measurements

A. Fabrication

The TSA was fabricated by CNC and the four ridges were assembled by using screws and fixtures. A flange was placed on the bottom of the TSA to fix the antenna on the rotator in the test chamber and on the probe antenna base. The EPP absorber was produced by mold fabrication.

B. Performance of the Low RCS TSA

The TSA and the absorber-integrated TSA have been measured in a far-field antenna chamber with 11 m length, as shown in Fig. 7. During the test, the ridge was placed parallel to horizontal plane of the chamber to ensure the test accuracy.

As show in Figs. 3 and 4, the measured results of the TSA fit well with the simulated results with slight disagreements. These disagreements may come from the simulation inaccuracy and measurement errors during the test. In addition, the absorber-integrated TSA showed little inconsistency between simulation and measurement, because of the inaccuracy of the absorber material, including permittivity, in simulation.

C. Reflectivity of the Low RCS TSA

As shown in Fig. 8, an arch-based reflectivity measurement instrument was used to measure the reflection coefficient of the TSA, the absorber-integrated TSA and the absorber reference. The normal incident reflection coefficient was measured by comparing the S_{11} of the absorber-integrated TSA to the S_{11} of a "perfect" reflection plate with same size of the sample. A large area of 600 mm height pyramidal absorbers was placed as a "nonreflected" background to minimize the ground reflection. Time gating can also be applied in the measurement to lower the noise from the reflection.

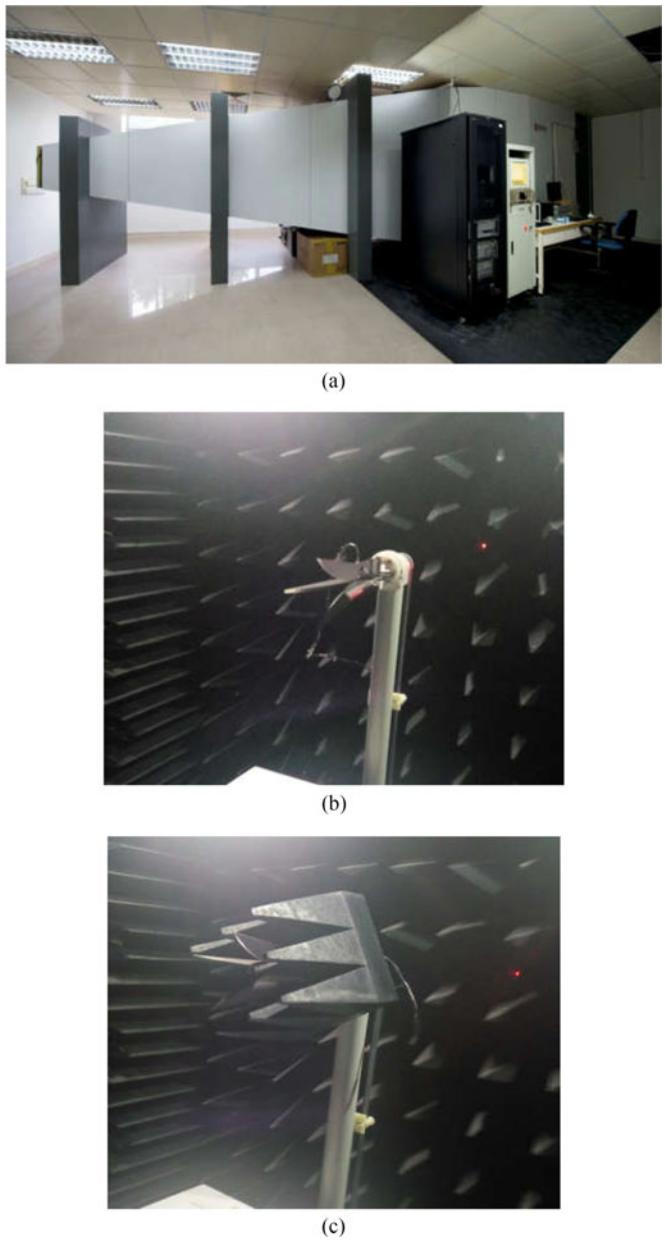

Fig. 7. Dart-9000 antenna chambers and measurement setup. (a) The front view of chamber. (b) The TSA test setup. (c) The TSA with absorber test setup.

In Fig. 5, the measurement showed the TSA had little impact on the performance of the absorbers, thus the distortion from this kind of probe antenna to the quiet zone of chambers is comparably small. The presence of the absorber greatly decreases the reflection coefficient of the TSA compared to the absorber-free TSA measurement, especially at high frequency. The discrepancy between simulation and measurement at lower

Fig. 8. Arch-based reflectivity test setup.

frequency from 0.6 to 1 GHz, may result from the small size of the test plate compared to the wavelength at these frequencies. And the difference at high frequencies comes from the inaccuracy of the simulation, because the simulation of very small signals (<–40 dB) at high frequencies usually spends a lot of computing resources and the results may be of high error.

D. RCS of the Low RCS TSA

The monostatic RCS of the absorber-integrated TSA and its absorber-free counterpart were measured in the RCS chamber in the tenth Research Institute of China Electronics Technology Group Corporation. The measurement covered from 1.1 to 5.85 GHz, and fits well with the simulation as shown in Fig. 6. The discrepancy between the simulation of the measurement of the absorber-integrated TSA may come from the inaccuracy of the absorber material parameters in the simulation, and from the RCS measurement uncertainties.

IV. Conclusion

In this paper, an absorber-integrated TSA design is presented as probe antennas for anechoic chambers. The proposed TSA was integrated with the EPP absorber. This mechanically robust RAM helps to precisely control the antenna properties and greatly reduce the reflection coefficient and the RCS of the proposed antenna covering a wideband frequency from 0.6 to 6 GHz. The good VSWR, stable gain, and low RCS have been achieved in the probe antenna, which makes it a better candidate for the anechoic chambers with higher requirement of quiet zone.

References

[1] CTIA, Washington, DC, USA. 2017. [Online]. Available: http://www.ctia.org

[2] 3GPP, Sophia Antipolis Cedex, France. 2017. [Online]. Available: http://www.3gpp.org

[3] W. Yu, Y. Qi, K. Liu, Y. Xu, and J. Fan, "Radiated two-stage method for LTE MIMO user equipment performance evaluation," *IEEE Trans. Electromagn. Compat.*, vol. 56, no. 6, pp. 1691–1696, Dec. 2014.

[4] P. Shen, Y. Qi, W. Yu, and F. Li, "Inverse matrix auto search technique for the RTS MIMO OTA test part1: Theory," *IEEE Trans. Electromagn. Compat*., vol. PP, no. 99, pp. 1–8, Jun. 2017.

[5] P. Shen, Y. Qi, W. Yu, F. Li, and J. Fan, "Fast and accurate TIS testing method for wireless user equipment with RSS reporting," *IEEE Trans. Electromagn. Compat.*, vol. 58, no. 3, pp. 887–895, Jun. 2016.

[6] Z. Liu, Y. Qi, F. Lin, W. Yu, J. Fan, and J. Chen, "Fast band-sweep total isotropic sensitivity measurement," *IEEE Trans. Electromagn. Compat.*, vol. 58, no. 4, pp. 1244–1251, Aug. 2016.

[7] P. Shen, Y. Qi, W. Yu, F. Li, and J. Fan, "Fast method for OTA performance testing of transmit-receive cofrequency mobile terminal," *IEEE Trans. Electromagn. Compat.*, vol. 58, no. 4, pp. 1367–1374, Aug. 2016.

[8] E. F. Knott, J. F. Shaeffer, and M. T. Tuley, *Radar Cross Sections*, 2nd ed. Raleigh, NC, USA: SciTech, 2004.

[9] T. Liu, X. Cao, J. Gao, Q. Zheng, W. Li, and H. Yang, "RCS reduction of waveguide slot antenna with metamaterial absorber," *IEEE Trans. Antennas Propag.*, vol. 61, no. 3, pp. 1479–1484, Mar. 2013.

[10] D. Pozar, "Radiation and scattering from a microstrip patch on a uniaxial substrate," *IEEE Trans. Antennas Propag.*, vol. AP–35, no. 6, pp. 613–621, Jun. 1987.

[11] P. J. Gibson, "The vivaldi aerial," in *Proc. 9th Eur. Microw. Conf.*, Brighton, U.K., 1979, pp. 101–105.

[12] J. D. Kraus, *Antennas*. New York, NY, USA: McGraw-Hill, 1950.

[13] Y. T. Jia, Y. Liu, S. Gong, T. Hong, and D. Yu, "Printed UWB end-fire vivaldi antenna with low RCS," *Prog. Electromagn. Res. Lett.*, vol. 37, pp. 11–20, 2013.

[14] H. K. Jang, W. J. Lee, and C. G. Kim, "Design and fabrication of a microstrip patch antenna with a low radar cross section in the X-band," *Smart Mater. Struct.*, vol. 20, 2011, Paper 015007.

[15] K. S. Cole and R. H. Cole, "Dispersion and absorption in dielectrics," *J. Chem. Phys.*, vol. 9, pp. 341–351, 1941.

Jiyu Wu (M'16) received the B.S. degree in electrical engineering from Southeast University, Nanjing, China, in 2010 and the M.S. degree in electrical and computer engineering from the University of Florida, Gainesville, FL, USA, in 2012. He is currently working toward the Ph.D. degree in electrical engineering at Hunan University, Changsha, China.

His research interests include the design of wideband antennas, millimeter-wave antennas, spiral antennas, loop antennas, and the design of antenna test systems and theory.

Mr. Wu received the Honorable Mention for the student paper competition in IEEE AP-S International Symposium on Antennas and Propagation in 2013.

Yihong Qi (M'92–SM'11) received the B.S. degree in electronics from the National University of Defense Technologies, Changsha, China, in 1982, and the M.S. degree in electronics from the Chinese Academy of Space Technology, Beijing, China, in 1985, and the Ph.D. degree in electronics from Xidian University, Xi'an, China, in 1989.

From 1989 to 1993, he was a Postdoctoral Fellow and then an Associate Professor with the Southeast University, Nanjing, China. From 1993 to 1995, he was a Postdoctoral Researcher at McMaster University, Hamilton, ON, Canada. From 1995 to 2010, he was with Research in Motion (Blackberry), Waterloo, ON, where he was the Director of Advanced Electromagnetic Research. He is currently the President and Chief Scientist with General Test Systems, Inc., Shenzhen, China; he founded DBJay in 2011, and he is the CTO of ENICE. He is also an Adjunct Professor in the EMC Laboratory, Missouri University of Science and Technology, Rolla, MO, USA, and an Adjunct professor in Hunan University, Changsha. He is an inventor of more than 200 published and pending patents.

Dr. Qi was a Distinguished Lecturer of IEEE EMC Society for 2014 and 2015, and serves as the Chairman of the IEEE EMC TC-12.

Wei Yu (M'13) received the B.S. degree in electrical engineering from Xi'an Jiaotong University, Xi'an, China, in 1991, the M.S. degree in electrical engineering from the China Academy of Space Technology, Beijing, China, in 1994, and the Ph.D. degree in electrical engineering from Xidian University, Xi'an, in 2000.

From 2001 to 2003, he was a Postdoctoral Fellow with the University of Waterloo, Canada. From 2008 to 2012, he was a CTO with Sunway Communications Ltd. He founded Antennovation Electronics, Inc., in 2004 and cofounded General Test Systems, Inc., Shenzhen, China, in 2012. He is now with DBJ Technologies as COO. He is an inventor of 32 published and pending patents. His current research interests include signal processing and mobile device test system.

Lie Liu (M'09–SM'12) received the B.Sc. degree from the Beijing University of Aeronautics and Astronautics (BUAA), Beijing, China, in 1991, and the M.Sc. degree from the China Academy of Launch-Vehicle Technology (CALT), Beijing, in 1994, and the Ph.D. degree from Nanyang Technological University, Singapore, in 2003.

From 2002 to 2012, he had been a Senior Research Scientist in Advanced Materials Group of Temasek Laboratories, National University of Singapore. Since 2015, he has been a Chief Technical Officer of General Test Systems, Shenzhen, China. He has published more than 50 papers in journals and conferences, and one book chapter. His research interests include EM materials, OTA measurement of wireless communication systems, and anechoic chamber design.

Fuhai Li (M'16) received the B.S. and M. S. degrees in instrument science and technology from Hunan University, Changsha, China, from 1982 to 1988.

He was a Professor with Hunan University. He had published more than 20 papers in the national core journals and involved the compiling of university teaching materials.

Mr. Li had several science and technology progress awards during his tenure at Hunan University. His students had lots of awards in kinds of national competitions under his leadership.